



Colorimetric captopril assay based on oxidative etching-directed morphology control of silver nanoprisms

Pu Zhang¹ · Li Wang² · Jing Zeng³ · Juan Tan³ · Yunfei Long⁴ · Yi Wang³ 

Received: 5 August 2019 / Accepted: 6 December 2019
© Springer-Verlag GmbH Austria, part of Springer Nature 2020

Abstract

Oxidative etching is an effective approach to control the morphology of nanomaterials. Taking silver nanocrystals (AgNCs) as an example, oxidative etching-directed morphological transformation from a triangular prism shape to a disk shape is achieved and then applied to the determination of captopril. As a mediator, trace amount of halides play important roles in the shape-controlled evolution of AgNCs. Etching causes the color of the triangular silver nanoprisms (AgNPRs) to change from blue to yellow on formation of round nanodisks. On addition of captopril, the oxidative etching of the AgNPRs is prevented owing to the protection by the drug via Ag-S bonding. In this case, the solution color does not change. This finding was used to design an assay of captopril that has a linear response in the 10–600 nM concentration range and a 2 nM limit of detection. This method also allows digital camera read-out. It was successfully applied to quality control of captopril in tablets.

Keywords Metal nanoparticles · Localized surface plasmon resonance · Smartphone · Peak shift · Hypertension · Pharmaceutical analysis

Introduction

Noble metal nanomaterials with unique localized surface plasmon resonance (LSPR) absorption have been widely used in optical sensing, catalysis, optical imaging, photothermal therapy and photovoltaic conversion [1–5]. Their LSPR can be well tailored since it has strong correlations to the size, geometric shape, composition and surface state of noble metal nanocrystals. Thus, controlling these parameters is significant for engineering their LSPR and thereby strengthening the

performance in various applications. Oxidative etching is one of the mightiest ways in the shape/crystallinity control of the noble metal nanoparticles. It refers to the zerovalent metal species such as atoms, clusters and nanocrystals are able to be oxidized back to metal ions in air with the aid of an etchant [6]. As a result, the type of crystal structure, morphological and size distributions of the final products can be altered. For example, Xia et al. found that the etchant of Cl^-/O_2 or $\text{Fe}^{3+}/\text{O}_2$ pair was able to remove metal seeds twin defects (e.g., Ag and Pd) that generated at the beginning of a synthesis. In that case, single-crystal nanoparticles would be the dominant products [7–9]. Yang et al. reported that oxidative etching exhibited specific selectivity toward different facets of anisotropy Ag nanocrystals since their surface energy was different. With increasing the concentration of an etchant (mixed NH_4OH and H_2O_2), Ag octahedrons transformed to concave octahedrons, and finally octapods [10]. Huang et al. successfully monitored the oxidative etching-mediated LSPR variation of single Au nanorods and Ag nanocubes using a dark-field microscope. Their studies demonstrated that corners with high surface energy are the preferential corrosion sites of anisotropy metal nanocrystals [11, 12]. Zhang et al. captured the etching process of Pd@Pt cubes in real-time via an in-situ transmission electron microscopy, where two different types of etching pathways were identified [13].

Electronic supplementary material The online version of this article (<https://doi.org/10.1007/s00604-019-4071-8>) contains supplementary material, which is available to authorized users.

✉ Yi Wang
ywang@cqu.edu.cn

¹ College of Pharmacy, Chongqing Medical University, Chongqing 400016, China

² Children's Hospital of Chongqing Medical University, Chongqing 400014, China

³ College of Chemistry, Chongqing Normal University, Chongqing 401331, China

⁴ School of Chemistry and Chemical Engineering, Hunan University of Science and Technology, Xiangtan 411201, Hunan, China

The concept of oxidative etching-directed morphology control of metal nanocrystals can also be applied in analytical chemistry. That is, morphology-dependent LSPR of metal nanoparticles can be well manipulated in the absence and presence of a specific etchant. In that case, analytical methods can be established according to the correlation of the LSPR and the etchant concentration (or the species that can consume/prevent the etchant). Several studies have used this strategy to achieve the determination of environmental contaminants [14], drugs [15], food additives [16], and biomarkers [17]. Compared with the widely used LSPR methods depending on the aggregation of metal nanoparticles, modifications on the surface of nanoparticles prior to detection is needless in the strategy involving oxidative etching-directed morphology control. In addition, the process of oxidative etching is able to be sensitively monitored by the LSPR variation of individual nanoparticles [18]. Nevertheless, it is still a great challenge to precisely manipulate the morphology and corresponding LSPR of metal nanocrystals through oxidative etching for the applications in analytical chemistry.

Herein, the LSPR of triangular Ag nanoprisms (AgNPRs) was precisely tuned by controlled oxidative etching, where the introduced trace amount of halide ions (e.g., Cl^-) played important role in this process. Specifically, the LSPR gradually blue shifted from ~ 660 nm to ~ 420 nm when the concentration of Cl^- increased, together with the change of solution color from blue to yellow. Interestingly, it was found that the oxidative etching toward AgNPRs was able to be prevented in the presence of captopril, which is a widely used drug for clinical treatment of hypertension and some types of congestive heart failure [19, 20]. Based on this finding, an LSPR method for the detection of captopril is developed. Compared with many other methods such as titration [21], fluorometry [22], voltammetry [23], chromatography [24] and colorimetry [25] for captopril assay, this approach exhibited the merits of high sensitivity, reliability and visualization. It has also been successfully applied in quality control of captopril in the pharmaceutical products. In addition, this method also allows smartphone read-out.

Experimental

Chemicals and materials

Chemical reagents including captopril, poly(vinyl pyrrolidone) (Mw, $\sim 10,000$), trisodium citrate and sodium borohydride were supplied by Aladdin Industrial Corporation (<http://www.aladdinreagent.com/>, Shanghai, China). Silver nitrate was supplied by Sinopharm Chemical Reagent Co., Ltd. (<http://www.sinoreagent.com/>, Shanghai, China). Potassium halides (KCl, KBr and KI), potassium nitrate and hydrogen peroxide were supplied by Kelong Chemical Co., Ltd. (<http://www.cdkelongchem.com/cn/>, Chengdu, China).

HEPES buffer (pH 7.0) and Milli-Q purified water ($18.2 \text{ M}\Omega\text{-cm}$) were used in the detection.

Instrumentations

A UV-vis spectrophotometer (Shimadzu UV-2550, Japan) was used to measure the extinction spectra of the Ag nanoparticles. A transmission electron microscope (Tecnai G2 F20, USA) was used to record the transmission electron microscopy (TEM) images of the particles under different conditions. An X-ray photoelectron spectrometer (Thermo ESCALAB 250, USA) was used to measure the X-ray photoelectron spectra (XPS). Dynamic light scattering (DLS) results were obtained by a Brookhaven Nano Brook omni (USA).

General procedure for determination of captopril

AgNPRs were synthesized refer to a reported reference with slight modification [26]. The details for the synthesis were shown in the [Supporting Information](#). For captopril assay, captopril standard solution (200 μL , with different concentrations) was mixed with 800 μL AgNPRs and 800 μL HEPES buffer (pH 7.0). Subsequently, 200 μL KCl (4 mM) was added in the mixture and incubated for 20 min at room temperature. Then, UV-vis spectra of the solutions were measured. To evaluate the quality of captopril tablets, pretreatment was carried out according to the Pharmacopeia of the People's Republic of China (Edition 2015) before assay (see [Supporting Information](#)).

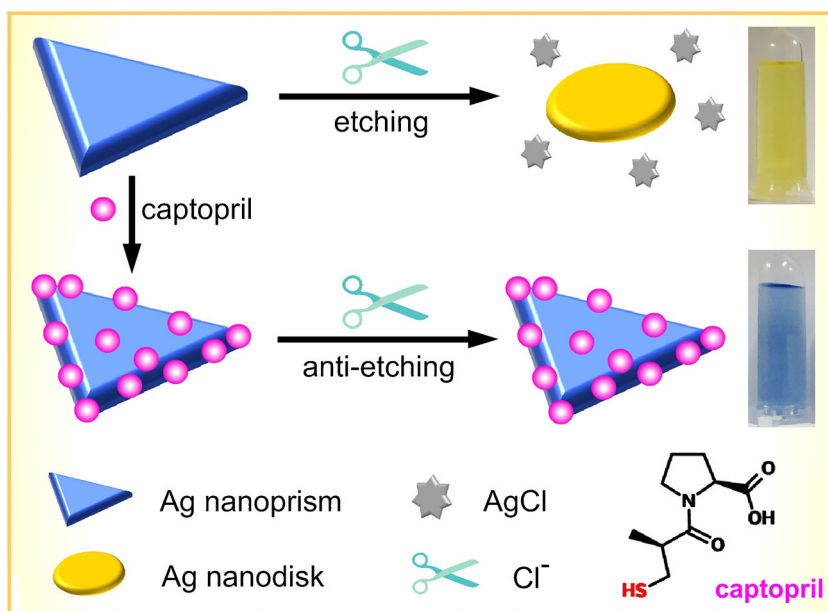
Results and discussion

Mechanism of the colorimetric assay

Scheme 1 generalizes the mechanism for captopril detection. Owing to the relatively high energy of the corners/edges of AgNPRs compared to their $\{111\}$ surfaces [27], Cl^- tends to primarily attack the corners/edges through oxidative etching. As a result, the AgNPRs with triangular shape would transform to smaller disc-shaped Ag nanoparticles. When captopril is introduced, it can bind on the surface of AgNPRs through Ag-S chemical bond since a thiol group is involved. Thus, captopril is able to protect AgNPRs against etching from chloride and thereby maintain the original morphology of triangular prism.

Such a mechanism is verified by UV-vis, TEM, XPS, and DLS studies. As known, the LSPR is closely related to the morphology of metal nanocrystals [28]. Herein, the morphological transform of Ag nanocrystals from triangular prism to round disk would cause the shift of their

Scheme 1 Diagrammatic drawing of the captopril assay based on oxidative etching-directed morphology control of AgNPRs



LSPR peak. As shown in Fig. 1, the AgNPRs can well disperse in water with a blue color of solution. Three characteristic peaks located at 331, 475, and 660 nm in the extinction spectrum (black line, a) are attributed to out-of-plane quadrupole, in-plane quadrupole, and in-plane dipole LSPR modes of AgNPRs, respectively [29]. With the addition of 0.4 mM Cl^- , the maximum LSPR peak of AgNPRs blue shifts from 660 to 440 nm (red line, b), accompanying with obvious change of solution color from blue to yellow. However, no obvious change of the LSPR wavelength is observed either in the presence of only captopril (green line, c) or the mix of 700 nM captopril and 0.4 mM Cl^- (blue line, d). In addition, the

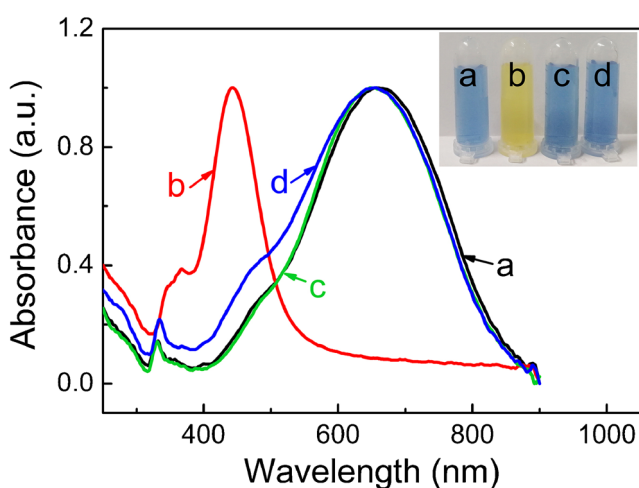


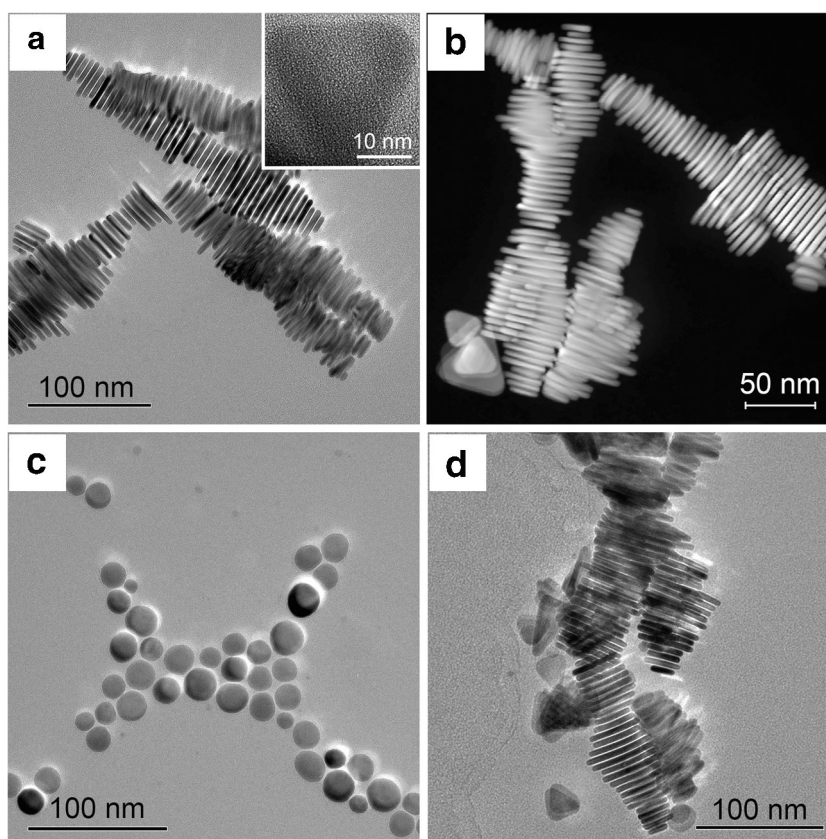
Fig. 1 Normalized LSPR spectra of AgNPRs under different conditions: **a** AgNPRs; **b** AgNPRs mixed with 0.4 mM Cl^- ; **c** AgNPRs mixed with 700 nM captopril (Cap); **d** AgNPRs mixed with 0.4 mM Cl^- and 700 nM captopril. Inset shows the corresponding colorimetric response of the solutions

mixed solutions of AgNPRs and captopril always kept initial blue color either with or without adding Cl^- , respectively. These observations demonstrates that captopril with thiol group has strong ability to prevent AgNPRs from oxidative etching by Cl^- .

The morphological transform of AgNPRs before and after incubation with the etchant and protective agent was further studied by TEM imaging. Figure 2a and b show that the initial AgNPRs are in uniform triangular plate-like shape. They have average edge length and thickness of 40 ± 7 and 5 ± 1.5 nm, respectively. It was found that the AgNPRs transformed to smaller round disk after interacting with 0.4 mM Cl^- , with average diameter of 24 ± 5 nm (Fig. 2c). However, the AgNPRs maintained their initial triangular plate-like shape when 700 nM captopril and 0.4 mM Cl^- were both present (Fig. 2d), confirming the protective effect of captopril toward etching. DLS data were also obtained to demonstrate the size change of AgNPRs after oxidative etching in solution. As shown in Fig. S1, the AgNPRs have an average hydrodynamic size of ~ 42 nm, which increased to ~ 165 nm after incubated with 0.4 mM Cl^- . The obvious size increase was attributed to the oxidative etching of AgNPRs to generate large amount of Ag^+ , and thereby formation of AgCl particles with large sizes finally. After incubation with captopril, the tendency of size increase was able to be prevented. Specifically, the size decreased to ~ 150 , ~ 63 and ~ 43 nm when 100, 400 and 700 nM of captopril was added, respectively. Although DLS data cannot reveal the actual size of the anisotropic AgNPRs, the results clearly indicate that the oxidative etching by Cl^- and no etching in the presence of captopril occurs in solution.

Apart from the TEM and DLS characterizations, XPS measurement was also carried out to explore the interaction between AgNPRs and captopril. High-resolution XPS spectra

Fig. 2 TEM images of **a, b** AgNPRs, **c** AgNPRs mixed with 0.4 mM Cl^- , and **d** AgNPRs mixed with 0.4 mM Cl^- and 700 nM captopril. Inset of **a** shows an individual AgNPR with triangular shape



indicated that the binding energies of Ag $3d_{5/2}$ and Ag $3d_{3/2}$ decreased from 367.9 to 367.3 eV and from 373.8 to 373.2 eV, respectively, after the AgNPRs interacted with captopril (Fig. S2). It suggested that part of the Ag atoms of AgNPRs were transformed into Ag^+ and formed Ag-S chemical bond [30]. The peak assigned to S 2p (160.8 eV) as shown in Fig. S3 further confirmed the existence of S on the surfaces of AgNPRs in the form of S^{2-} [31]. According to previously reports, citrate that introduced in the synthesis of AgNPRs can bind more strongly to base $\{111\}$ facets than other facets of fcc Ag [32]. In this case, the etchant Cl^- would preferentially attack the higher-energy corners and edges (i.e., side $\{100\}$ facets). Thus, rounded disks with smaller sizes were obtained after etching. When captopril was added into the system, captopril would preferentially bind to side $\{100\}$ facets of the AgNPRs since citrate can effectively prevent captopril from binding on the $\{111\}$ facets. Therefore, even very small amounts of captopril can play a significant role in the protection of AgNPRs against oxidative etching, and thus high sensitivity of the captopril detection can be achieved.

Studies on the detection conditions

Reaction conditions in solution can significantly affect the oxidative etching process. Thus, different

morphologies and thereby the LSPR of the Ag nanoparticles would be obtained under different detection conditions. First, the influence of Cl^- amount on controlled etching was investigated. Figure 3a shows that the LSPR peak of AgNPRs gradually moves to shorter wavelengths with rising the Cl^- amount from 0 to 0.4 mM, and almost keeps constant when the concentration is larger than 0.4 mM. It suggests that all the AgNPRs have been transformed into smaller round disks with relatively low surface energy when the concentration of Cl^- reaches 0.4 mM, and thus the oxidative etching will not continue at this time. Except for Cl^- , the oxidative etching of other halide ions toward AgNPRs was also investigated. It was found that the peak of AgNPRs also moved to the wavelengths shorter than 500 nm when 0.4 mM KBr and KI were introduced, respectively. A control group with the addition of 0.4 mM KNO_3 showed no obvious peak shift, which excluded the influence of K^+ on the oxidative etching (Fig. S4). The average hydrodynamic sizes of the particles were also obviously increased in the presence of Br^- or I^- , which was consistent with that of Cl^- . However, when the same concentration of KNO_3 was present, variation of hydrodynamic size was not observed (Fig. S5). These results prove again that halide

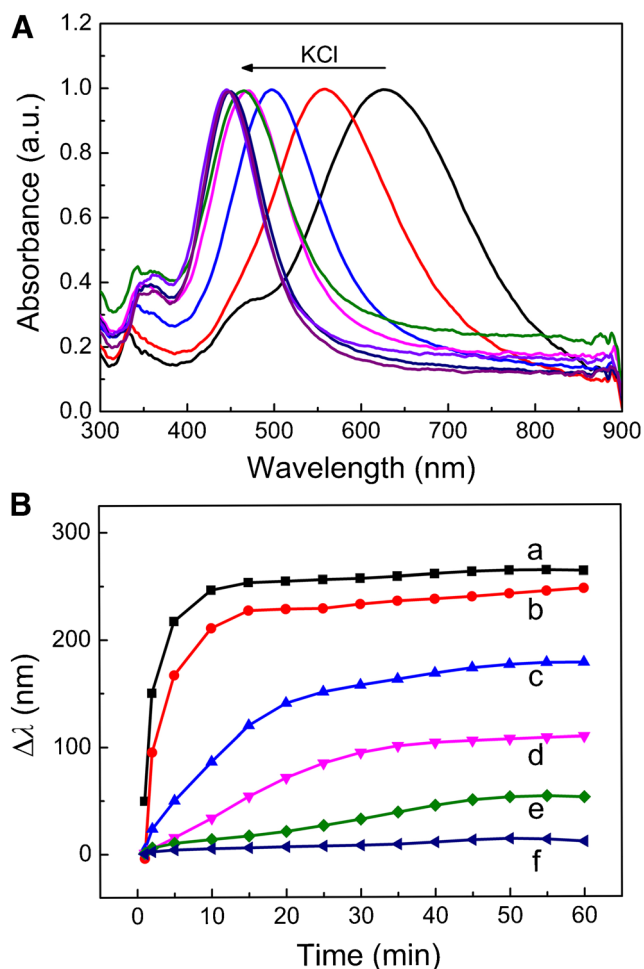


Fig. 3 Influences of different conditions on the system. **a** Normalized LSPR spectra of AgNPRs in the presence of different amounts of Cl^- 0 to 0.5 mM. **b** Reaction kinetics in the absence and presence of different amounts of captopril. Concentrations of captopril: (a) 0, (b) 100, (c) 300, (d) 500, (e) 600, and (f) 700 nM

ions are responsible for the oxidative etching in air and thus the morphological evolution.

Reaction kinetics of the oxidative etching and captopril-involved non-etching were also inspected. Figure 3b exhibited that the LSPR of AgNPRs blue shifted more than ~200 nm within the initial 10 min in the presence of only Cl^- , and did not change any more thereafter. However, the reaction kinetics and final degree of peak shift ($\Delta\lambda$) both decreased when Cl^- and captopril were added, which further decreased as the concentration of captopril increased. The typical LSPR evolution of AgNPRs in the presence of both 0.4 mM Cl^- and 300 nM captopril was shown in Fig. S6. For all the reactions with the addition of different concentrations of captopril, the LSPR peaks of Ag nanocrystals have no longer moving after 30 min. It suggests that the detection can be completed no more than half an hour.

Determination of captopril through LSPR evolution

On the basis of the oxidative etching-directed morphology control of AgNPRs and their LSPR evolution, we further established a colorimetric method for quantitative assay of captopril. As shown in Fig. 4a, the LSPR peak of AgNPRs blue shifted to ~440 nm after etching by 0.4 mM Cl^- in the absence of captopril. However, constant red shift of the peak occurred with increasing captopril from 10 to 700 nM. The peak almost moved back to that of the initial AgNPRs in the presence of 700 nM captopril. Correlation of the LSPR evolution ($\Delta\lambda$) and captopril concentration (c_{Cap}) was fitted as a standard plot for determination (Fig. 4b). A detectable range of 10–600 nM ($r = 0.9934$) with a detection limit of 2 nM ($3\sigma/k$) was obtained. The sensitivity of this method is higher than that of many previous reports for captopril assay (Table S1).

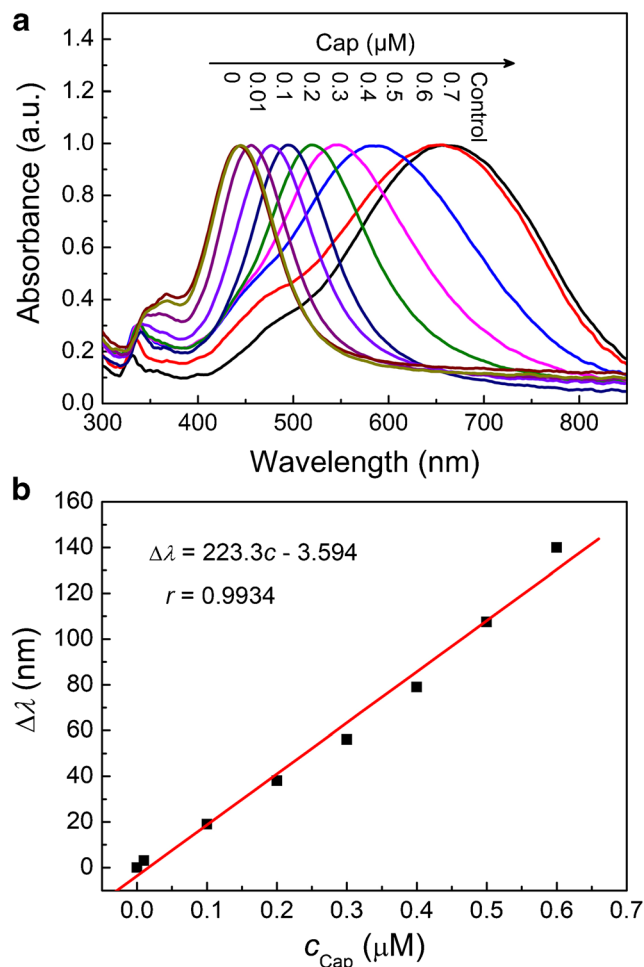


Fig. 4 **a** Normalized LSPR spectra of AgNPRs together with 0.4 mM Cl^- and different concentrations of captopril (0–700 nM). **b** Calibration plot for the determination of captopril

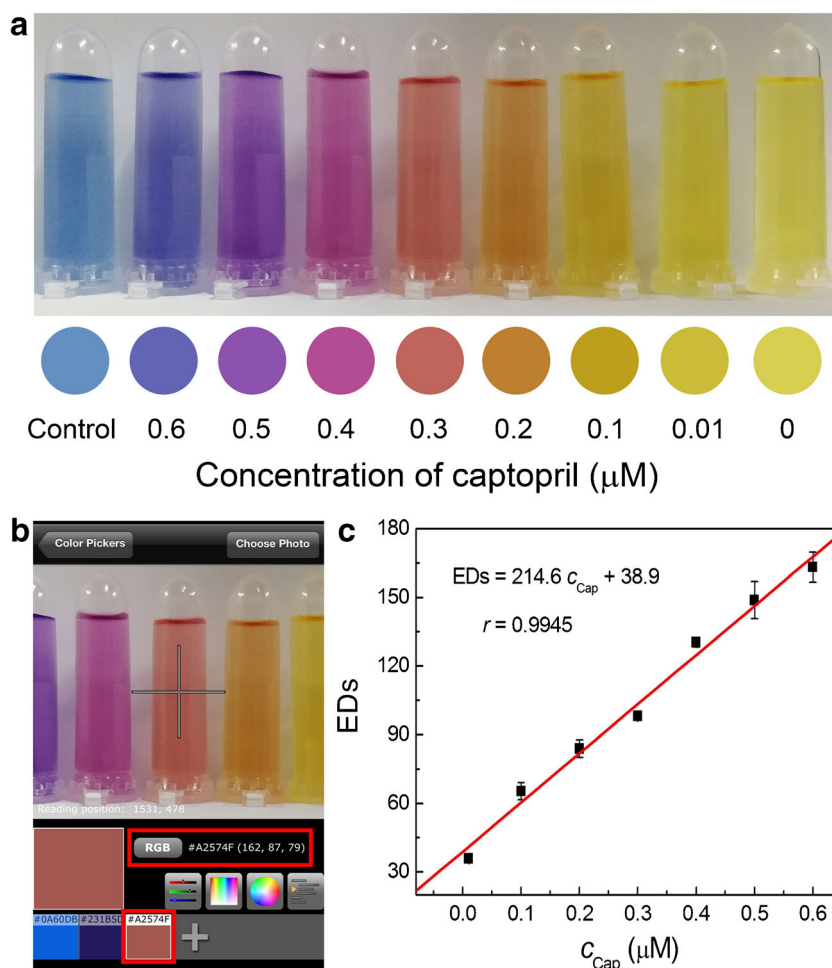
Digital camera-based captopril assay

To avoid the use of specialized instruments for detection, a smartphone was also employed as a portable device to record and analyze the data. Firstly, a representative photograph of AgNPR solutions in the presence of different amounts of captopril (0–600 nM) was captured by a smartphone. Figure 5a displays the color change of solution from yellow, orange, red, to purple, and finally close to blue of the initial AgNPRs as the concentration of captopril increases. Then, the RGB (three-primary colors) values of each sample was read out and analyzed by an open source app (called *Color Pickers*) that loaded in the smartphone (Fig. 5b). The Euclidean distance [ED = $(\Delta R^2 + \Delta G^2 + \Delta B^2)^{1/2}$] was employed to quantitatively illustrate the color change of solution [33]. As shown in Fig. 5c, linear enhancement of the EDs was observed as the concentration of captopril increased from 10 to 600 nM ($r = 0.9945$). Obviously, the resolution of a smartphone is quite better than that of visual detection. Taken together, colorimetric determination of captopril is able to be carried out by this approach using either UV–vis spectrophotometer or smartphone as an analyzer.

Selectivity and interference studies

Selectivity and interference studies of this approach to detect captopril was carried out. Common species in pharmaceutical products such as inorganic ions, saccharides and other pharmaceutical adjuvants were inspected in the detection. In these experiments, the concentration of other species (100 μM) was more than 100 times higher than that of captopril (700 nM). Figure 6a shows that the peak shifts more than 250 nm in the presence of captopril, while less than 20 nm replaced by other investigated species. The solutions in the absence (control group, only AgNPRs and Cl^-) and presence of other interfering species all exhibited yellow color, while blue color appeared only in the presence of captopril (inset of Fig. 6a). Except for selectivity study, potential interfering substances were also mixed with captopril in each sample before detection. As shown in Fig. 6b, compared with that of the control group only containing captopril (300 nM), the $\Delta\lambda$ of other samples all fluctuated within 10%, where more than 100 times of interfering species coexisted with captopril. Since the detection is dependent on the prevention of etching via Ag-S bonding, biothiols (e.g., cysteine and glutathione) will also

Fig. 5 Smartphone-based method for captopril assay: **a** a photograph of the solutions containing different amounts of captopril (0–600 nM); **b** screen capture by a smartphone app for captopril assay; **c** Plot of EDs versus captopril concentration



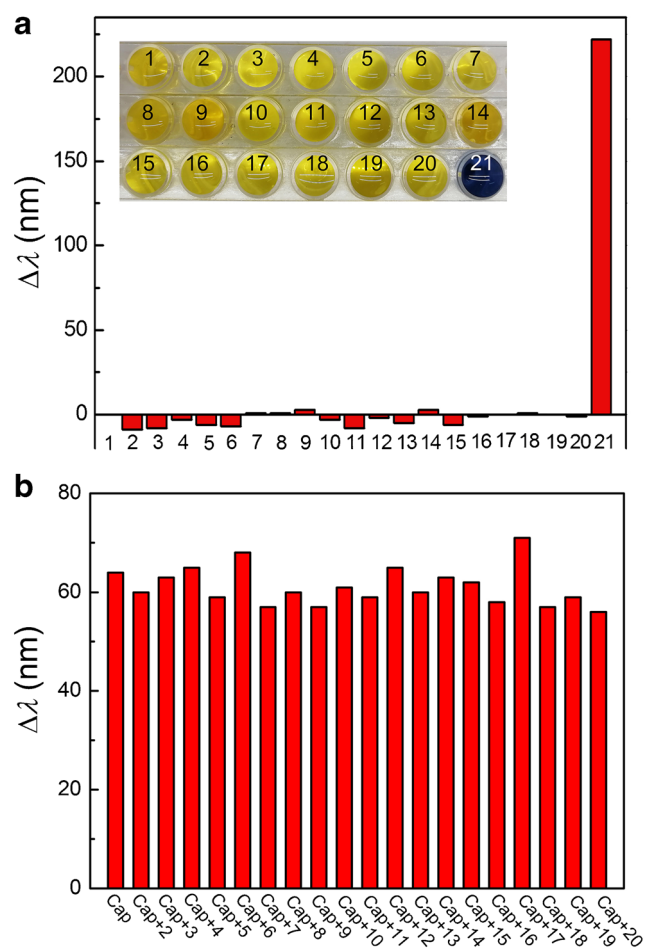


Fig. 6 Selectivity and interference studies. **a** LSPR peak shift ($\Delta\lambda$) of AgNPRs after mixing with 0.4 mM Cl^- (sample 1) and captopril (700 nM, sample 21) or other potential interfering substances (100 μM for samples 2–19, 50 $\mu\text{g}/\text{mL}$ for sample 20). Inset shows the corresponding colorimetric response of the sample solutions. **b** LSPR peak shift ($\Delta\lambda$) of AgNPRs after incubating with 0.4 mM Cl^- in the presence of 300 nM captopril (control group) and the mix of captopril (300 nM) together with other potential interfering substances (100 μM for samples 2–19, 50 $\mu\text{g}/\text{mL}$ for sample 20), respectively. The interfering substances added in samples 2–20 are ethanol, $\text{Na}_2\text{C}_2\text{O}_4$, Na_2CO_3 , NaHCO_3 , CH_3COONa , $\text{Pb}(\text{NO}_3)_2$, CuSO_4 , $\text{Al}(\text{NO}_3)_3$, $\text{Mg}(\text{NO}_3)_2$, glucose, citric acid, polyvinyl pyrrolidone, ethylenediaminetetraacetic acid disodium salt, α -cyclodextrin, β -cyclodextrin, sucrose, carboxymethyl cellulose, D-mannitol, and starch, respectively

Table 1 Determination of captopril in tablets

Sample	Labeled (nM)	Detected (nM)	Added (nM)	Found (nM)	Recovery (%)	RSD ($n=3$, %)
Tablet 1 ^a	100.0	97.6	100.0	94.0	94.0	7.94
			150.0	154.0	102.7	4.74
			200.0	204.3	102.1	5.95
Tablet 2 ^b	100.0	95.8	100.0	100.5	100.5	6.20
			150.0	145.9	97.3	1.93
			200.0	207.5	103.8	4.06

^a purchased from Beijing Jingfeng Pharmaceutical Co., Ltd., China

^b purchased from Shanxi Jinhua Huixing Pharmaceutical Co., Ltd., China

have response and thus interfere the captopril assay. Hence, this method can be applied to quality control of captopril in pharmaceutical products while is not suitable to detect captopril in body fluids (e.g., blood samples). This will be one of the major limitations of this method.

Quantitation of captopril in tablets

Quality control of captopril in tablets was further conducted to testify the accuracy and potential applications of this method. The tablets with main ingredient of captopril were purchased from two different manufacturers in China. Table 1 shows the results of captopril concentration measured by this method, which are identical with the labeled contents. Besides, satisfied spiked recoveries of 94.0–103.8% were also gained. These results confirmed the feasibility and reliability of this approach for determination of drugs containing captopril.

Conclusions

A sensitive colorimetric method for the determination of captopril has been developed using an etching strategy, where the etching-directed morphological transformation of Ag nanoparticles from triangular prism to rounded disk can be effectively prevented by captopril. The detection can proceed rapidly, with a detectable range of 10–600 nM of captopril. It has been successfully applied to the determination of captopril in tablets. We believe that the strategy of controlled etching of metal nanoparticles can be extended to other systems for sensing. Biothiols will also respond to this method and interfere. Thus, this method will be good for quality control of captopril in pharmaceutical products while not suitable to detect captopril in body fluids.

Acknowledgements This work was sponsored by the National Natural Science Foundation of China (No. 21775014 and 81972020). Y. W. was also sponsored by the Chongqing High-level Personnel of Special Support Program (Youth Top-notch Talent). P. Z. was also sponsored by the Chongqing Talent Program (Youth Top-notch Talent).

References

- Rycenga M, Copley CM, Zeng J, Li W, Moran CH, Zhang Q, Qin D, Xia Y (2011) Controlling the synthesis and assembly of silver nanostructures for plasmonic applications. *Chem Rev* 111:3669–3712
- He R, Wang Y-C, Wang X, Wang Z, Liu G, Zhou W, Wen L, Li Q, Wang X, Chen X, Zeng J, Hou JG (2014) Facile synthesis of pentacle gold–copper alloy nanocrystals and their plasmonic and catalytic properties. *Nat Commun* 5:4327
- Lei G, Gao PF, Yang T, Zhou J, Zhang HZ, Sun SS, Gao MX, Huang CZ (2017) Photoinduced electron transfer process visualized on single silver nanoparticles. *ACS Nano* 11:2085–2093
- Yang L, Zhen SJ, Li YF, Huang CZ (2018) Silver nanoparticles deposited on graphene oxide for ultrasensitive surface-enhanced Raman scattering immunoassay of cancer biomarker. *Nanoscale* 10:11942–11947
- Wang Y, Zhang P, Fu W, Zhao Y (2018) Morphological control of nanoprobe for colorimetric antioxidant detection. *Biosens Bioelectron* 122:183–188
- Zheng Y, Zeng J, Ruditskiy A, Liu M, Xia Y (2014) Oxidative etching and its role in manipulating the nucleation and growth of noble-metal nanocrystals. *Chem Mater* 26:22–33
- Wiley B, Herricks T, Sun Y, Xia Y (2004) Polyol synthesis of silver nanoparticles: use of chloride and oxygen to promote the formation of single-crystal, truncated cubes and tetrahedrons. *Nano Lett* 4:1733–1739
- Xiong Y, Chen J, Wiley B, Xia Y (2005) Understanding the role of oxidative etching in the polyol synthesis of Pd nanoparticles with uniform shape and size. *J Am Chem Soc* 127:7332–7333
- Ma Y, Li W, Zeng J, McKiernan M, Xie Z, Xia Y (2010) Synthesis of small silver nanocubes in a hydrophobic solvent by introducing oxidative etching with Fe(III) species. *J Mater Chem* 20:3586–3589
- Mulvihill MJ, Ling XY, Henzie J, Yang P (2010) Anisotropic etching of silver nanoparticles for plasmonic structures capable of single-particle SERS. *J Am Chem Soc* 132:268–274
- Wang Y, Zou HY, Huang CZ (2015) Real-time monitoring of oxidative etching on single Ag nanocubes via light-scattering dark-field microscopy imaging. *Nanoscale* 7:15209–15213
- Zhang HZ, Li RS, Gao PF, Wang N, Lei G, Huang CZ, Wang J (2017) Real-time dark-field light scattering imaging to monitor the coupling reaction with gold nanorods as an optical probe. *Nanoscale* 9:3568–3575
- Shan H, Gao W, Xiong Y, Shi F, Yan Y, Ma Y, Shang W, Tao P, Song C, Deng T, Zhang H, Yang D, Pan X, Wu J (2018) Nanoscale kinetics of asymmetrical corrosion in core-shell nanoparticles. *Nat Commun* 9:1011
- Yang R, Song D, Wang C, Zhu A, Xiao R, Liu J, Long F (2015) Etching of unmodified Au@Ag nanorods: a tunable colorimetric visualization for the rapid and high selective detection of Hg²⁺. *RSC Adv* 5:102542–102549
- Lee H-C, Chen T-H, Tseng W-L, Lin C-H (2012) Novel core etching technique of gold nanoparticles for colorimetric dopamine detection. *Analyst* 137:5352–5357
- Wang G-L, Zhu X-Y, Jiao H-J, Dong Y-M, Wu X-M, Li Z-J (2012) “Oxidative etching-aggregation” of silver nanoparticles by melamine and electron acceptors: an innovative route toward ultrasensitive and versatile functional colorimetric sensors. *Anal Chim Acta* 747:92–98
- Zhang Z, Chen Z, Wang S, Cheng F, Chen L (2015) Iodine-mediated etching of gold nanorods for plasmonic ELISA based on colorimetric detection of alkaline phosphatase. *ACS Appl Mater Interfaces* 7:27639–27645
- Xie T, Jing C, Ma W, Ding Z, Gross AJ, Long Y-T (2015) Real-time monitoring for the morphological variations of single gold nanorods. *Nanoscale* 7:511–517
- Mullane KM, Moncada S (1980) Prostacyclin mediates the potentiated hypotensive effect of bradykinin following captopril treatment. *Eur J Pharmacol* 66:355–365
- Hansson L, Lindholm LH, Niskanen L, Lanke J, Hedner T, Niklason A, Luomanmäki K, Dahlöf B, Faire U, Mörlin C, Karlberg BE, Wester PO, Björck JE (1999) Effect of angiotensin-converting-enzyme inhibition compared with conventional therapy on cardiovascular morbidity and mortality in hypertension: the captopril prevention project (CAPPP) randomised trial. *Lancet* 353:611–616
- Schmidt E Jr, Melchert WR, Rocha FRP (2009) Flow-injection iodimetric determination of captopril in pharmaceutical preparations. *J Braz Chem Soc* 20:236–242
- Xiao SJ, Zhao XJ, Chu ZJ, Xu H, Liu GQ, Huang CZ, Zhang L (2017) New off-on sensor for captopril sensing based on photoluminescent MoOx quantum dots. *ACS Omega* 2:1666–1671
- Armijo F, Torres I, Tapia R, Molero L, Antilén M, Río R, Valle MA, Ramírez G (2010) Captopril electrochemical oxidation on fluorine-doped SnO₂ electrodes and their determination in pharmaceutical preparations. *Electroanalysis* 22:2269–2276
- Vancea S, Imre S, Donáth-Nagy G, Béla T, Nyulas M, Muntean T, Borka-Balás R (2009) Determination of free captopril in human plasma by liquid chromatography with mass spectrometry detection. *Talanta* 79:436–441
- Ravazzi CG, Franco MOK, Vieira MCR, Suarez WT (2018) Smartphone application for captopril determination in dosage forms and synthetic urine employing digital imaging. *Talanta* 189:339–344
- Zhang Q, Li N, Goebel J, Lu Z, Yin Y (2011) A systematic study of the synthesis of silver nanoplates: is citrate a “magic” reagent? *J Am Chem Soc* 133:18931–18939
- Zeng J, Tao J, Su D, Zhu Y, Qin D, Xia Y (2011) Selective sulfuration at the corner sites of a silver nanocrystal and its use in stabilization of the shape. *Nano Lett* 11:3010–3015
- Wiley BJ, Im SH, Li Z-Y, McLellan J, Siekkinen A, Xia Y (2006) Maneuvering the surface plasmon resonance of silver nanostructures through shape-controlled synthesis. *J Phys Chem B* 110:15666–15675
- Millstone JE, Hurst SJ, Metraux GS, Cutler JJ, Mirkin CA (2009) Colloidal gold and silver triangular nanoprisms. *Small* 5:646–661
- Han Y, Lupitsky R, Chou T-M, Stafford CM, Du H, Sukhishvili S (2011) Effect of oxidation on surface-enhanced Raman scattering activity of silver nanoparticles: a quantitative correlation. *Anal Chem* 83:5873–5880
- Djoković V, Krsmanović R, Božanić DK, McPherson M, Tendeloo GV, Nair PS, Georges MK, Radhakrishnan T (2009) Adsorption of sulfur onto a surface of silver nanoparticles stabilized with sago starch biopolymer. *Colloids Surf B-Biointerfaces* 73:30–35
- Zeng J, Xia X, Rycenga M, Henneghan P, Li Q, Xia Y (2011) Successive deposition of silver on silver nanoplates: lateral versus vertical growth. *Angew Chem Int Ed* 50:244–249
- Li L, Zhang L, Zhao Y, Chen Z (2018) Colorimetric detection of Hg(II) by measurement the color alterations from the “before” and “after” RGB images of etched triangular silver nanoplates. *Microchim Acta* 185:235

Publisher's note Springer Nature remains neutral with regard to jurisdictional claims in published maps and institutional affiliations.